

Background

The doubly-imaged lens JVAS B0218+357 has the smallest angular image-separation (~ 330 mas) amongst the known galactic-scale lens systems [see Fig (1)]. The lensed object is a blazar ($z = 0.944$, Cohen et al. 2003) with a typical core-jet morphology and a frequency-dependent structure, and the lens is believed to be a spiral galaxy ($z = 0.685$, Browne et al. 1993). A robust confirmation of the latter is provided by the recent HST-ACS image of this system with a very high resolution and sensitivity (York et al. 2005), which clearly shows the two point images and the underlying spiral structure of the lens galaxy.

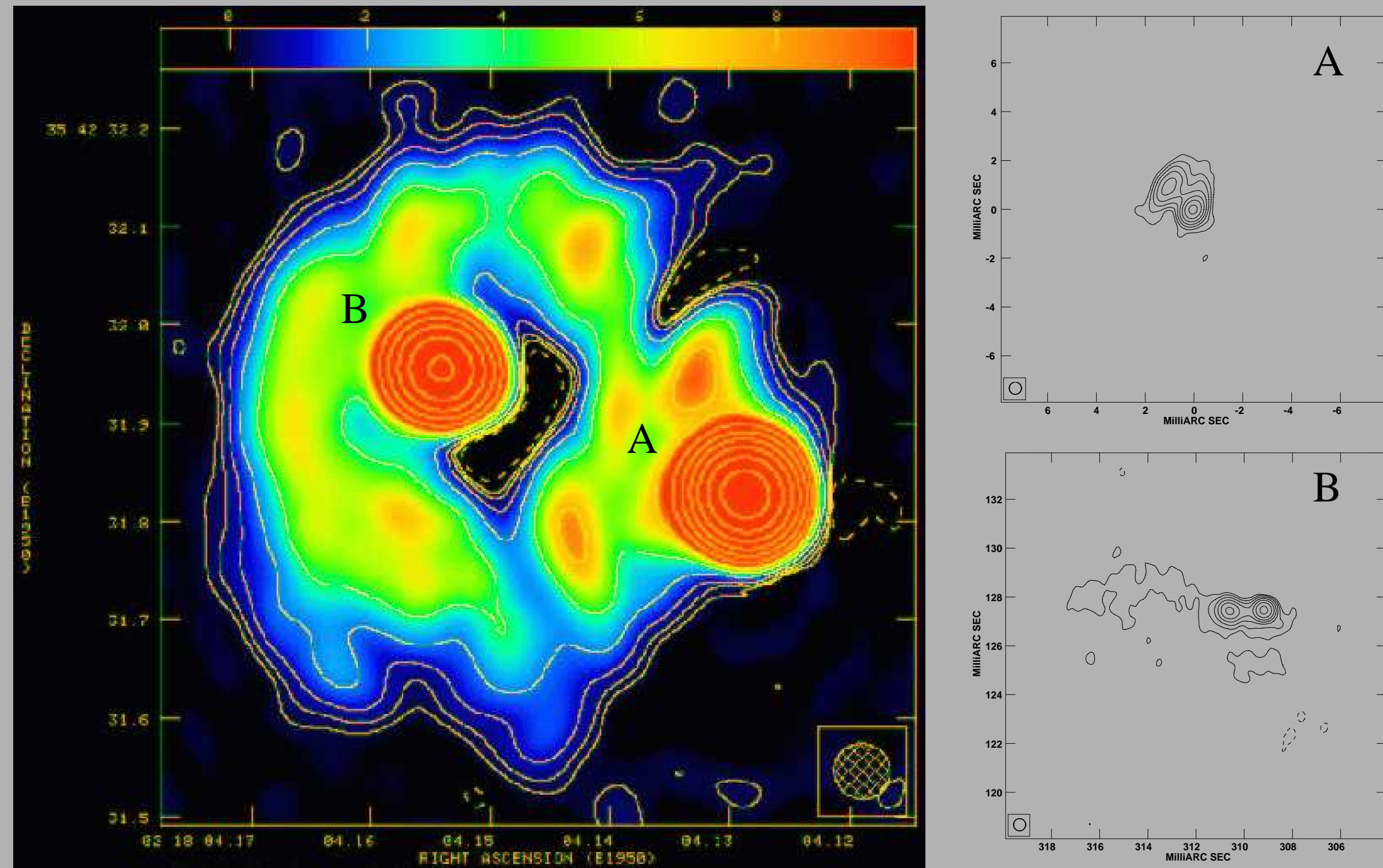


Figure 1: Left: 5 GHz map of the lens from combined MERLIN and VLA data (Wucknitz 2002). Right: VLBI 15-GHz map of B0218+357 for image A (top) and B (bottom), plotted with a restoring beam of 0.5 mas.

All the observed characteristics of this lens system, such as the lens-geometry and the image positions, can be reconstructed well using a simple lens-model, except the image flux-density ratios. The anomaly, addressed and discussed extensively by Mittal et al. (2006, hereafter M06), is manifested in the steady decline in the image flux-density ratio (A/B) from 4 to 2 with decreasing radio frequencies from ~ 20 GHz to 1 GHz, which violates the achromatic nature of the phenomenon of GL. In M06, the authors used the technique of inverse phase-referencing to discard the gradient in the image-magnification ratio across the images as a cause of the flux ratio anomaly in B0218+357.

In this work, we seek other explanations for the flux ratio anomaly in B0218+357, of entirely different origins. These are free-free absorption and scattering, and are assumed to occur under the hypothesis of a molecular cloud residing in the lens galaxy along the line-of-sight to image A. The analyses were carried out based on the multi-frequency VLBI observations of this lens system, which are presented in M06. Here, we focus only on the first mechanism and show that free-free absorption due to an HII region covering the entire structure of image A at 1.65 GHz can explain the image flux ratio anomaly.

Free-free absorption

There are numerous line observations in B0218+357 (e.g. Combes & Wiklind 1998) that indicate evidence of large amounts of molecular gas and HI in the lens galaxy. It has been shown that these lines arise solely due to image A (Carilli et al. 2000; Menten & Reid 1996), which is in agreement with a strong relative extinction also observed in this image (Falco et al. 1999). The interpretation of these facts is that there is a molecular cloud directly in front of image A (Henkel et al. 2005; Falco et al. 1999).

Free-free absorption requires regions of plasma along the lines-of-sight to the image in consideration. The presence of a molecular cloud in front of image A provides an easy solution to this requirement as molecular clouds harbour sites of recent star formation, which through photoionization build up regions of ionized hydrogen around them. Based on the Singular Isothermal Elliptical Potential (SIEP) as the lens model, image A lies at a projected distance of 2 kpc from the lens centre. Its line-of-sight may well pass through one of the spiral arms of the galaxy, which are known to harbour extensive star forming regions.

Assuming a state of Local Thermodynamic Equilibrium, the intensity of background radiation that passes through an HII region is modified according to the law of radiative transfer to

$$I_{\text{ff}}(\nu, \tau) = I_0(\nu) e^{-\tau_{\text{ff}}(\nu)}, \quad (1)$$

where $\tau_{\text{ff}}(\nu)$ is the optical depth,

$$\tau_{\text{ff}} = 3.19 \times 10^{-7} \left(\frac{T_e}{10^4 \text{ K}} \right)^{-1.35} \left(\frac{EM}{\text{cm}^{-6} \text{ pc}} \right) \left(\frac{\nu}{\text{GHz}} \right)^{-2.1}. \quad (2)$$

Here, EM is the Emission Measure.

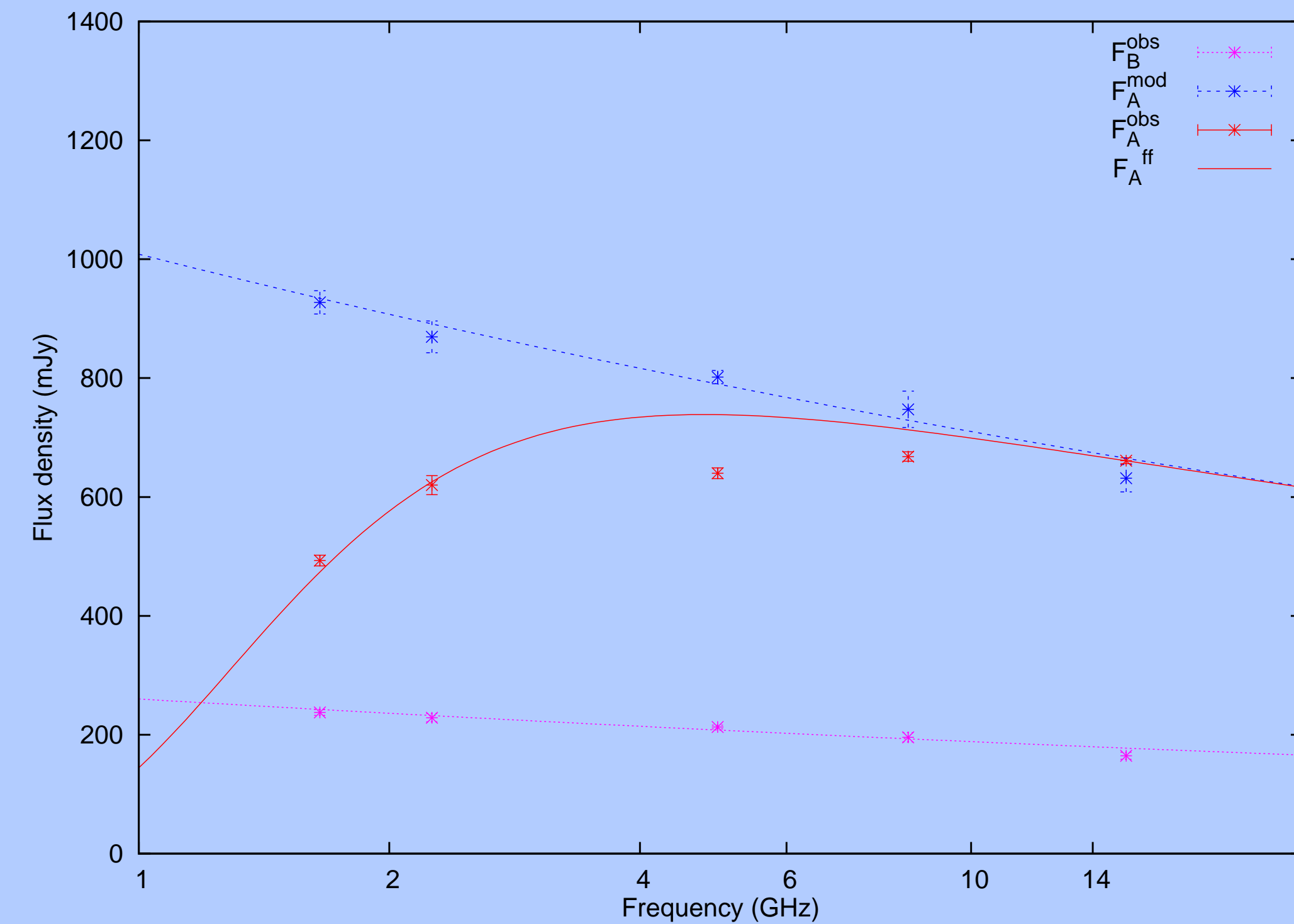
Parameter Estimation of the HII region

Assuming the spectrum of image B to reflect the true source spectrum, i.e. free from non-gravitational perturbations, and using the SIEP lens model, the true spectrum of image-A can be determined from the measured flux-densities of image A. Further, with the help of Eq. (2) and from the knowledge of the original and the modified spectrum of image A, the curve given by Eq. (1) can be fitted to the observed flux-densities at different frequencies to determine the best fitting values of the plasma parameters.

The parameters of the hypothesized HII region were estimated by approximating the spectra of image B and the modelled image A by a synchrotron power-law,

$$F_A(\nu) \propto \nu^{-a}; F_B(\nu) \propto \nu^{-b}, \quad (3)$$

where $F_A(\nu)$ is the image A flux-density and $F_B(\nu)$ is the image B flux-density, and $a = 0.153 \pm 0.018$ and $b = 0.147 \pm 0.022$ are the power law indices fitted to their spectra. Substituting $F_A(\nu)$ for $I_0(\nu)$ in Eq. (1), the best-fitting value for EM can be calculated using the χ^2 minimization method to minimize the difference between the observed and the modelled image A flux-densities. Shown in Fig. 2 are the flux densities of image A (blue crosses) modelled using the observed flux densities of image B (pink crosses). The FFA curve (red curve) is fitted to the observed flux-densities of image A (red crosses). The various parameters, including the electron densities for different values of L , estimated for two values of temperatures are given in Table 1.



The values of EM , although quite large, are consistent with those measured in giant Galactic HII regions, and the estimations of n_e and L are also in good agreement with those observed for Galactic and extragalactic HII regions. In the present context the most meaningful combination of n_e and L is the last entry in Table 1 for both T values. This is because we have assumed that the HII region covers all of image A, which at 1.65 GHz (the lowest frequency) has a deconvolved size of ~ 28 mas which translates into a physical size of about 200 pc at the redshift of the lens galaxy. Such giant (and supergiant) HII regions, although not ubiquitous, have indeed been observed, both as galactic and extragalactic. For example, the giant HII region complex W49 in the Milky Way Galaxy has $L = 150$ pc and $n_e = 100 \text{ cm}^{-3}$, NGC 604 in M33 has $L = 400$ pc and $n_e \leq 60 \text{ cm}^{-3}$ and NGC 5471 in M101 has $L = 800$ pc and $n_e = 200 \text{ cm}^{-3}$ (Shields 1990).

T (K)	EM ($\text{cm}^{-6} \text{ pc}$)	L (pc)	n_e (cm^{-3})	
10^4	$(1.8 \pm 0.3) \times 10^7$	1	0.15	4243
		10	1.5	1342
		100	14	424
		200	28	300
4 000	$(5.3 \pm 0.9) \times 10^6$	1	0.15	2302
		10	1.5	728
		100	14	230
		200	28	163

Table 1: The parameters derived for the HII region in front of image A. T is the temperature and EM is the emission measure of the HII region. Given also are the various combinations of the electron density and the depth of the cloud for given emission measures.

From this it can be concluded that the free-free absorption hypothesis is capable of reproducing the observed spectrum of image A and, thereby, of solving the image flux-density ratio anomaly in B0218+357. Furthermore, the values of the emission measure resulting from the fit for two extreme electron temperatures are quite reasonable in that similar values have been measured for Galactic and extragalactic HII regions, lending further support to the hypothesis.

Conclusions

We have shown that the image flux ratio anomaly in B0218+357 can be explained by invoking propagation effects, namely those arising due to free-free absorption, which is thought to occur in an ionized medium of the lens galaxy (Mittal et al. 2007).

As a separate issue, we also investigated whether there is any evidence of a contribution from scattering in the lens galaxy to the disagreement between the predicted and the observed image flux-density ratios. We found that, first, there is no evidence of ν -dependent image-broadening for image A. Second, even though the estimated scattering measures are within the observed range of scattering measures in other systems, the back-projected component-size in image A and the size of the scattering disk are not compatible with each other at all (five) frequencies. Thus, it seems that scattering is not a satisfactory explanation for the flux ratio anomaly seen in B0218+357.

A multi-frequency VLBI analysis of B0218+357 has led us to conclude that in order to investigate the causes of flux ratio anomalies evident in numerous lens systems, a multi-frequency approach is most yielding. Further, we note that in order to use image flux-density ratios measured at radio wavelengths as constraints for lens modelling, the most trust-worthy values are those measured at high frequencies (such as 15 GHz and above) since the propagation effects at these frequencies are minimal.

References

- Browne, I. W. A. et al. 1993, MNRAS, 263, 32
 Carilli, C. L. et al. 2000, Phy. Rev. Letters, 85, 5511
 Cohen, J. G. et al. 2003, ApJ, 583, 67
 Combes, F. & Wiklind, T. 1998, A&A, 334, L81
 Falco, E. E. et al. 1999, ApJ, 523, 617
 Henkel, C. et al. 2005, A&A, 440, 893
 Menten, K. M. & Reid, M. J. 1996, ApJ, 465, L99
 Mittal, R. et al. 2006, A&A, 447, 515
 —. 2007, A&A, 465, 405
 Shields, G. A. 1990, ARA&A, 28, 525
 Wucknitz, O. 2002, Ph.D. Thesis
 York, T. et al. 2005, MNRAS, 357, 124